

Parameterizations and Lagrange Cubics for Fitting Multidimensional Data

R. Kozera^{1,2,3}, L. Noakes² and M. Wilkołazka³

¹ Warsaw University of Life Sciences - SGGW
Institute of Information Technology
Ul. Nowoursynowska 157, 02-776 Warsaw, Poland
ryszard.kozera@sggw.pl
ryszard.kozera@gmail.com

² The University of Western Australia
Faculty of Engineering and Mathematical Sciences
35 Stirling Highway, Crawley, W.A. 6009 Perth, Australia
lyle.noakes@uwa.edu.au

³ The John Paul II Catholic University of Lublin
Faculty of Natural and Health Sciences
Ul. Konstantynów 1H, 20-708 Lublin, Poland
magda.wilkolazka@gmail.com
magda8310@kul.lublin.pl

Abstract

This paper discusses the issue of interpolating data points in arbitrary Euclidean space with the aid of Lagrange cubics $\hat{\gamma}^L$ and exponential parameterization. The latter is commonly used to either fit the so-called reduced data $Q_m = \{q_i\}_{i=0}^m$ for which the associated exact interpolation knots remain unknown or to model the trajectory of the curve γ passing through Q_m . The exponential parameterization governed by a single parameter $\lambda \in [0, 1]$ replaces such discrete set of unavailable knots $\{t_i\}_{i=0}^m$ ($t_i \in I$ - an internal clock) with some new values $\{\hat{t}_i\}_{i=0}^m$ ($\hat{t}_i \in \hat{I}$ - an external clock). In order to compare γ with $\hat{\gamma}^L$ the selection of some $\phi : I \rightarrow \hat{I}$ should be predetermined. For some applications and theoretical considerations the function $\phi : I \rightarrow \hat{I}$ needs to form an *injective mapping* (e.g. in length estimation of γ with any $\hat{\gamma}$ fitting Q_m). We formulate and prove two *sufficient conditions* yielding ϕ as *injective* for given Q_m and analyze their asymptotic character which forms an important question for Q_m getting sufficiently dense. The *algebraic conditions* established herein are also *geometrically visualized* in 3D plots with the aid of *Mathematica*. This work is supplemented with illustrative examples including numerical testing of the underpinning convergence rate in length estimation $d(\gamma)$ by $d(\hat{\gamma})$ (once $m \rightarrow \infty$). The *reparameterization* has potential ramifications in computer graphics and robot navigation for trajectory planning e.g. to construct a new curve $\tilde{\gamma} = \hat{\gamma} \circ \phi$ controlled by the appropriate choice of interpolation knots and of mapping ϕ (and/or possibly Q_m).

1 Introduction

Assume that $\gamma : I \rightarrow \mathbb{E}^n$ represents a smooth *regular curve* (i.e. $\dot{\gamma}(t) \neq \vec{0}$) of class C^k (usually with $k = 3, 4$) defined over a compact interval $I = [0, T]$ (with $0 < T < \infty$). Suppose that $m + 1$ interpolation points $\{q_i\}_{i=0}^m = \{\gamma(t_i)\}_{i=0}^m$ (forming the so-called *reduced data* Q_m) belong to an arbitrary Euclidean space \mathbb{E}^n . Here $\mathcal{T} = \{t_i\}_{i=0}^m$ is not given. We introduce now (see e.g. [1], [7], [12] or [19]) some preliminary notions (applicable for $m \rightarrow \infty$).

Definition 1.1. The interpolation knots \mathcal{T} are *admissible* if:

$$\lim_{m \rightarrow \infty} \delta_m \rightarrow 0, \text{ where } \delta_m = \max_{1 \leq i \leq m} \{t_i - t_{i-1} : i = 1, 2, \dots, m\}. \quad (1)$$

Definition 1.2. The interpolation knots \mathcal{T} are *more-or-less uniform* if there exist constants $0 < K_l \leq K_u$ such that:

$$(K_l/m) \leq t_i - t_{i-1} \leq (K_u/m), \quad (2)$$

for all $i = 1, 2, \dots, m$ and any $m \in \mathbb{N}$. Alternatively, more-or-less uniformity amounts to the existence of some constant $0 < \beta \leq 1$ such that $\beta\delta_m \leq t_i - t_{i-1} \leq \delta_m$ for all $i = 1, 2, \dots, m$ and arbitrary $m \in \mathbb{N}$. Lastly, the subfamily \mathcal{T}_{β_0} of more-or-less uniform samplings represents a set of β_0 -*more-or-less uniform* samplings if each of its representatives satisfies $\beta_0 \leq \beta \leq 1$, for some $0 < \beta_0 \leq 1$ fixed.

Having selected the fitting scheme $\hat{\gamma}$ of Q_m the unknown knots \mathcal{T} for the interpolant $\hat{\gamma}$ must somehow be replaced by estimates $\hat{\mathcal{T}} = \{\hat{t}_i\}_{i=0}^m$ subject to $\hat{\gamma}(\hat{t}_i) = q_i$. We use here the so-called *exponential parameterization* (see e.g. [17]) which depends on a single parameter $\lambda \in [0, 1]$ according to:

$$\hat{t}_0 = 0 \quad \text{and} \quad \hat{t}_i = \hat{t}_{i-1} + \|q_i - q_{i-1}\|^\lambda, \quad (3)$$

for $i = 1, 2, \dots, m$. It is also assumed here that $q_i \neq q_{i+1}$ so that the extra condition $\hat{t}_i < \hat{t}_{i+1}$ is preserved as stipulated generically while fitting reduced data Q_m . The case of $\lambda = 0$ in (3) gives *uniform knots* $\hat{t}_i = i$. Evidently the latter does not reflect the geometry of Q_m . On the other hand, $\lambda = 1$ yields the so-called *cumulative chord parameterization* which coincides with Euclidean distances between consecutive points q_i and q_{i+1} and as such it refers to the spread of Q_m . More information on the above topic and related issues can be found e.g. in [3], [5], [16], [17] or [18].

The selection of the specific interpolant $\hat{\gamma} : \hat{I} = [0, \hat{T}] \rightarrow \mathbb{E}^n$ (with $\hat{T} = \hat{t}_m$) together with some knots' estimates $\hat{\mathcal{T}} \approx \mathcal{T}$ raises an important question concerning the convergence rate (if any) in approximating γ with $\hat{\gamma}$ (or its length) once $m \rightarrow \infty$. Recall first (see [1], [12] or [19]):

Definition 1.3. Consider a family $\{F_{\delta_m}, \delta_m > 0\}$ of functions $F_{\delta_m} : I \rightarrow \mathbb{E}^n$. We say that F_{δ_m} is of order $O(\delta_m^\alpha)$ (denoted as $F_{\delta_m} = O(\delta_m^\alpha)$), if there is a constant $K > 0$ such that, for some $\bar{\delta} > 0$ the inequality $\|F_{\delta_m}(t)\| < K\delta_m^\alpha$ holds for all $\delta_m \in (0, \bar{\delta})$, uniformly over I .

For a given $\hat{\gamma}$ fitting dense data Q_m based on $\hat{\mathcal{T}} \approx \mathcal{T}$ (and some *a priori* selected mapping $\phi : I \rightarrow \hat{I}$) the natural question arises about the distance measurement $\|F_{\delta_m}\| = \|\gamma - \hat{\gamma} \circ \phi\|$ tending to 0 (uniformly over I), while $m \rightarrow \infty$. Of course, by (1) proving $F_{\delta_m} = \gamma - \hat{\gamma} \circ \phi = O(\delta_m^\alpha)$ not only guarantees the latter but also establishes lower bound on convergence speed. The coefficient α appearing in Def. 1.3 is called *the convergence rate* in approximating γ by $\hat{\gamma} \circ \phi$ uniformly over $[0, T]$. If additionally such α cannot be improved (once γ and \mathcal{T} are given) then α is *sharp*. The latter analogously extends to the length estimation (with $n = 1$), for which the scalar expression $F_{\delta_m} = d(\gamma) - d(\hat{\gamma}) = O(\delta_m^\beta)$ is to be considered.

For certain applications such as the analysis of the convergence rate in $d(\gamma) = \int_0^T \|\dot{\gamma}(t)\| dt \approx d(\hat{\gamma}) = \int_0^{\hat{T}} \|\dot{\hat{\gamma}}(\hat{t})\| d\hat{t}$ (see e.g. [2], [5] or [15]) the mapping $\phi(t) = \hat{t}$ should be a *reparameterization* of I into \hat{I} (i.e. $\dot{\phi} > 0$). In other situations such as robot's and drone path planning the extra trajectory looping of $\hat{\gamma}$ is sometimes needed (e.g. for traction line posts' inspection while making circles by drone). Of course, in many other applications robot navigation requires trajectory planning with no loops whatsoever. In that context (as well as for length estimation) one of the conditions to exclude the local looping of $\hat{\gamma} \circ \phi$ is to require ϕ to be an *injective* function (see e.g. [13]).

From now on it is assumed that $\hat{\gamma} = \hat{\gamma}^L$ which represents a piecewise-Lagrange cubic $\hat{\gamma}^L : \hat{I} = [0, \hat{T}] \rightarrow \mathbb{E}^n$ (see e.g. [1]). More precisely, the interpolant $\hat{\gamma}^L$ is defined as a *track-sum* of Lagrange cubics $\{\hat{\gamma}_{i=3k}^L\}_{k=0}^{m/3}$ with each $\hat{\gamma}_i^L : \hat{I}_i = [\hat{t}_i, \hat{t}_{i+3}] \rightarrow \mathbb{E}^n$ satisfying $q_{i+j} = \hat{\gamma}_i^L(\hat{t}_{i+j})$, for

$j = 0, 1, 2, 3$. As already pointed out the unavailable knots \mathcal{T} are estimated with $\hat{\mathcal{T}}$ governed by exponential parameterization (3). For simplicity we suppose that $m = 3k$, where $k \in \mathbb{N}$. In a similar fashion, one selects here $\phi = \psi^L$ defined as a *track-sum* of Lagrange cubics $\{\psi_{i=3k}^L\}_{k=0}^{m/3}$ mapping $\psi_i^L : I_i = [t_i, t_{i+3}] \rightarrow [\hat{t}_i, \hat{t}_{i+3}]$ and fulfilling $t_{i+j} = \hat{\psi}_i^L(t_{i+j})$, for $j = 0, 1, 2, 3$. Evidently if $\hat{\psi}_i^L > 0$ (as $\hat{t}_i < \hat{t}_{i+1}$) then $\psi_i^L : I_i \rightarrow \hat{I}_i = Rg(\psi_i^L)$ (here $Rg(\psi_i^L)$ denotes the range of ψ_i^L). On the other hand if ψ_i^L is not injective we may also have $\psi_i^L : I_i \rightarrow \hat{I}_i \subset Rg(\psi_i^L)$. In order to construct the composition $\hat{\gamma}_i^L \circ \psi_i^L$ as a well-defined function, each domain of $\hat{\gamma}_i^L$ is here understood as naturally extendable from \hat{I}_i to \mathbb{R} . Such adjusted Lagrange piecewise-cubics denoted as $\hat{\gamma}_i^L$ satisfy $\hat{\gamma}_i^L|_{\hat{I}_i} = \hat{\gamma}_i^L$. The following result holds (see e.g. [7], [9] or [19]):

Theorem 1.4. *Assume $\gamma \in C^4([0, T])$ be a regular curve in \mathbb{E}^n sampled admissibly (see (1)). For $\hat{\gamma}^L$ and $\lambda = 1$ in (3) each mapping ψ_i^L is a C^∞ reparameterization of I_i into \hat{I}_i and we have (uniformly over $[0, T]$):*

$$\gamma - \hat{\gamma}_i^L \circ \psi_i^L = O(\delta_m^4). \quad (4)$$

In the remaining cases of $\lambda \in [0, 1)$ from (3) let γ be sampled more-or-less uniformly (see (2)). Then for each mapping ψ_i^L combined with $\hat{\gamma}_i^L$ the following holds (uniformly over $[0, T]$):

$$\gamma - \hat{\gamma}_i^L \circ \psi_i^L = O(\delta_m). \quad (5)$$

Both (4) and (5) are *sharp within the class* of $\gamma \in C^4([0, T])$ and *within a given family of admitted samplings*, assumed here as either (1) or (2), respectively. By the latter we understand the existence of at least one $\gamma_0 \in C^4([0, T])$ and some admissible (or more-or-less uniform) sampling \mathcal{T}_0 for which $\alpha(1) = 4$ in (4) (or $\alpha(\lambda) = 1$ for $\lambda \in [0, 1)$ in (5)) are sharp according to Def. 1.3 - see also [9] or [12]. Note that ψ^L as a *track-sum* of $\{\psi_{i=3k}^{m/3}\}$ defines a piecewise C^∞ mapping of I into \mathbb{R} at least continuous at \mathcal{T} . If ψ^L is a reparameterization (e.g. always holding asymptotically for $\lambda = 1$) then $\psi^L : I \rightarrow \hat{I}$. In particular for $\lambda = 1$ we also have $d(\gamma) - d(\hat{\gamma}^L) = O(\delta_m^4)$ - see [19]. In contrast, the injectivity of ψ_i^L and length estimation for $\lambda \in [0, 1)$ has not been so far examined.

In this paper we introduce *two sufficient conditions enforcing* each $\psi_i^L : I_i \rightarrow \hat{I}_i$ to be *injective*, for $\lambda \in [0, 1)$ governing the exponential parameterization (3). These two conditions are represented by the inequalities (6) and (7). In the next step, Th. 2.1 is established (*the main result of this paper*) to formulate several sufficient conditions enforcing (6) and (7) to hold asymptotically. Noticeably all derived conditions stipulating asymptotically the injectivity of ψ^L are independent from γ and apply to any fixed $\lambda \in [0, 1)$ and to any preselected β_0 -more-or-less-uniform samplings (i.e. to any $0 < \beta_0 < 1$ fixed *a priori*). Additionally, all re-transformed *algebraic constraints* established here are *visualized* with the aid of 3D plots in *Mathematica* (see [22]). The conditions can also be exploited once the incomplete information about samplings is available such as *a priori* knowledge of the respective upper and lower bounds for each triples (M_{im}, N_{im}, P_{im}) characterizing \mathcal{T} as specified in (8) - see also Rem. 3.1. The examples illustrate Th. 2.1 and the relevance of this work (see Ex. 1). The conjecture concerning the sharp convergence rate $\alpha(\lambda) = 2$ in length estimation $d(\gamma) - d(\hat{\gamma}^L) = O(\delta_m^{\alpha(\lambda)})$ (combined with (3) for all $\lambda \in [0, 1)$ yielding $\hat{\phi} > 0$) is tested numerically (see Ex. 2 and Rem. 3.2).

2 Sufficient Conditions for Injectivity of ψ_i^L

In this section we establish and discuss the asymptotic character (i.e. applicable for m sufficiently large) of two sufficient conditions enforcing ψ_i^L to be a *genuine reparameterization* of I_i into \hat{I}_i based on multidimensional reduced data Q_m .

Evidently the positivity of the quadratic $\psi_i^L(t) = a_i t^2 + b_i t + c_i$ over I_i is e.g. guaranteed (for both *sparse* and *dense* data Q_m) provided if e.g. either (6) or (7) hold:

$$a_i < 0 \quad \text{and} \quad \psi_i^L(t_i) > 0 \quad \text{and} \quad \psi_i^L(t_{i+3}) > 0, \quad (6)$$

$$a_i > 0 \quad \text{and} \quad \psi_i^L\left(-\frac{b_i}{2a_i}\right) > 0. \quad (7)$$

Noticeably, any admissible sampling (1) can be characterized as follows:

$$t_{i+1} - t_i = M_{im}\delta_m, \quad t_{i+2} - t_{i+1} = N_{im}\delta_m \quad \text{and} \quad t_{i+3} - t_{i+2} = P_{im}\delta_m, \quad (8)$$

where $0 < M_{im}, N_{im}, P_{im} \leq 1$. The main theoretical contribution of this paper reads as:

Theorem 2.1. *Let $\gamma \in C^3$ be sampled β_0 -more-or-less uniformly (see Def. (1.2)) with knots \mathcal{T} represented by (8). For data Q_m combined with exponential parameterization (3) (with any fixed $\lambda \in [0, 1)$) the condition (6) yielding each $\psi_i^L : I \rightarrow \hat{I}_i$ as a reparameterization holds asymptotically, if the following three inequalities are satisfied for sufficiently large m :*

$$\frac{1}{P_{im} + N_{im} + M_{im}} \left(\frac{P_{im}^{\lambda-1} - N_{im}^{\lambda-1}}{P_{im} + N_{im}} - \frac{N_{im}^{\lambda-1} - M_{im}^{\lambda-1}}{N_{im} + M_{im}} \right) \leq \rho < 0, \quad (9)$$

$$M_{im}^{\lambda-1} - \frac{(N_{im}^{\lambda-1} - M_{im}^{\lambda-1})M_{im}}{N_{im} + M_{im}} + \frac{(P_{im}^{\lambda-1} - N_{im}^{\lambda-1})M_{im}(N_{im} + M_{im})}{(P_{im} + N_{im})(P_{im} + N_{im} + M_{im})} - \frac{(N_{im}^{\lambda-1} - M_{im}^{\lambda-1})M_{im}}{P_{im} + N_{im} + M_{im}} \geq \rho_1 > 0, \quad (10)$$

$$P_{im}^{\lambda-1} - \frac{(N_{im}^{\lambda-1} - M_{im}^{\lambda-1})P_{im}(P_{im} + N_{im})}{(N_{im} + M_{im})(P_{im} + N_{im} + M_{im})} + \frac{P_{im}(P_{im}^{\lambda-1} - N_{im}^{\lambda-1})}{P_{im} + N_{im} + M_{im}} + \frac{P_{im}(P_{im}^{\lambda-1} - N_{im}^{\lambda-1})}{P_{im} + N_{im}} \geq \rho_2 > 0, \quad (11)$$

with fixed $\rho < 0$, $\rho_1 > 0$ and $\rho_2 > 0$ but arbitrary small. Similarly, the condition (7) enforcing $\psi_i^L > 0$ holds asymptotically if the following two inequalities are met for sufficiently large m :

$$\frac{1}{P_{im} + N_{im} + M_{im}} \left(\frac{P_{im}^{\lambda-1} - N_{im}^{\lambda-1}}{P_{im} + N_{im}} - \frac{N_{im}^{\lambda-1} - M_{im}^{\lambda-1}}{N_{im} + M_{im}} \right) \geq \rho_3 > 0, \quad (12)$$

$$\begin{aligned} M_{im}^{\lambda-1} + \frac{(N_{im}^{\lambda-1} - M_{im}^{\lambda-1})(2N_{im} + M_{im})}{3(N_{im} + M_{im})} \\ - \frac{(N_{im}^{\lambda-1} - M_{im}^{\lambda-1})^2}{3(N_{im} + M_{im})} \cdot \frac{(P_{im} + N_{im})(P_{im} + N_{im} + M_{im})}{(P_{im}^{\lambda-1} - N_{im}^{\lambda-1})(N_{im} + M_{im}) - (N_{im}^{\lambda-1} - M_{im}^{\lambda-1})(P_{im} + N_{im})} \\ - \left[\frac{(P_{im}^{\lambda-1} - N_{im}^{\lambda-1})(N_{im} + M_{im}) - (N_{im}^{\lambda-1} - M_{im}^{\lambda-1})(P_{im} + N_{im})}{(N_{im} + M_{im})(P_{im} + N_{im})(P_{im} + N_{im} + M_{im})} \right] \frac{(N_{im}^2 + N_{im}M_{im} + M_{im}^2)}{3} \end{aligned} \geq \rho_4 > 0, \quad (13)$$

where constants $\rho_3 > 0$ and $\rho_4 > 0$ are fixed and small.

Proof. Newton interpolation formula (see [1]) based on divided differences of ψ_i^L yields over I_i :

$$\psi_i^L(t) = \psi_i^L(t_i) + \psi_i^L[t_i, t_{i+1}](t - t_i) + \psi_i^L[t_i, t_{i+1}, t_{i+2}](t - t_i)(t - t_{i+1}) + \psi_i^L[t_i, t_{i+1}, t_{i+2}, t_{i+3}],$$

which for each $t \in I_i$ renders $\psi_i^L(t) =$

$$\begin{aligned} & \psi_i^L[t_i, t_{i+1}] + \psi_i^L[t_i, t_{i+1}, t_{i+2}](2t - t_i - t_{i+1}) \\ & + \psi_i^L[t_i, t_{i+1}, t_{i+2}, t_{i+3}]((t - t_{i+1})(t - t_{i+2}) + (t - t_i)(t - t_{i+2}) + (t - t_i)(t - t_{i+1})). \end{aligned} \quad (14)$$

We recall now the proof of (18) (see [9] or [12]) since it is vital for further arguments. As γ is regular it can be assumed to be parameterized by *arc-length* rendering $\|\dot{\gamma}(t)\| = 1$, for $t \in [0, T]$ (see [2]). The latter due to $1 \equiv \|\dot{\gamma}(t)\|^2 = \langle \dot{\gamma}(t) | \dot{\gamma}(t) \rangle$ results in $0 \equiv (\|\dot{\gamma}(t)\|^2)' = 2\langle \dot{\gamma}(t) | \ddot{\gamma}(t) \rangle$ over $t \in [0, T]$. The orthogonality of $\dot{\gamma}$ and $\ddot{\gamma}$ nullifies certain terms in the expression (for $j = i + k$ with $k = 0, 1, 2$ and any $\lambda \in [0, 1]$):

$$\hat{t}_{j+1} - \hat{t}_j = \|q_{j+1} - q_j\|^\lambda = \|\gamma(t_{j+1}) - \gamma(t_j)\|^\lambda = \langle \gamma(t_{j+1}) - \gamma(t_j) | \gamma(t_{j+1}) - \gamma(t_j) \rangle^\lambda \quad (15)$$

once Taylor expansion for $\gamma \in C^3$ is used:

$$\gamma(t_{j+1}) - \gamma(t_j) = (t_{j+1} - t_j)\dot{\gamma}(t_j) + \frac{(t_{j+1} - t_j)^2}{2}\ddot{\gamma}(t_j) + O((t_{j+1} - t_j)^2). \quad (16)$$

Indeed, upon substituting (16) into (15) and exploiting $\langle \dot{\gamma}(t) | \ddot{\gamma}(t) \rangle = 0$ one obtains:

$$\hat{t}_{j+1} - \hat{t}_j = (t_{j+1} - t_j)^\lambda (1 + O((t_{j+1} - t_j)^2))^{\frac{\lambda}{2}}. \quad (17)$$

For any admissible samplings the constants in the term $O((t_{j+1} - t_j)^2)$ depend on the third derivative of γ which is bounded over $[0, T]$ as $\gamma \in C^3$. Again Taylor Th. applied to the function $f(x) = (1 + x)^{\frac{\lambda}{2}}$ at $x_0 = 0$ yields for all $x \in [-\varepsilon, \varepsilon] = I_\varepsilon$ (with some fixed $\varepsilon > 0$) the existence of some ξ_x satisfying $|\xi_x| < |x|$ such that $f(x) = 1 + \frac{\lambda}{2}x + \frac{\lambda}{4}(\frac{\lambda}{2} - 1)(1 + \xi_x)^{\frac{\lambda}{2} - 2}$. For $0 < \varepsilon < 1$ we exclude the singularity of $\tau(\xi_x) = (1 + \xi_x)^{\frac{\lambda}{2} - 2}$ at $\xi_x = -1$ (with $\lambda \in [0, 1]$) which forces τ to be bounded over I_ε . Thus for $|\xi_x| < |x| \leq \varepsilon < 1$ we have $f_1(x) = 1 + \frac{\lambda}{2}x + O(x^2)$ - the constant standing along x^2 depends now on λ (which is fixed). Take now $x = O((t_{j+1} - t_j)^2)$ determined in (17) which is asymptotically small (for m large) due to the admissibility condition (1) and thus separated from -1 . Hence the second-divided differences of ψ_i^L satisfy (with $k = 0, 1, 2$):

$$\psi_i^L[t_{i+k}, t_{i+k+1}] = \frac{\hat{t}_{i+k+1} - \hat{t}_{i+k}}{t_{i+k+1} - t_{i+k}} = (t_{i+k+1} - t_{i+k})^{\lambda-1} + O((t_{i+k+1} - t_{i+k})^{1+\lambda}). \quad (18)$$

Thus, by (8) and (18) one obtains for each $\lambda \in [0, 1]$ and $k = 0, 1, 2$ the following formula for the *second divided differences* of ψ_i^L (needed also in (14)):

$$\psi_i^L[t_{i+k}, t_{i+k+1}] = R_{imk}^{\lambda-1} \delta_m^{\lambda-1} + O(\delta_m^{1+\lambda}), \quad (19)$$

with $R_{im0} = M_{im}$, $R_{im1} = N_{im}$ and $R_{im2} = P_{im}$. Furthermore still by (18) combined with $0 < (t_{i+l+1} - t_{i+l})(t_{i+2} - t_i)^{-1} \leq 1$ (for $l = 0, 1$) and telescoped $t_{i+2} - t_i = (t_{i+2} - t_{i+1}) + (t_{i+1} - t_i)$ the third-divided difference of ψ_i^L is equal to $\psi_i^L[t_i, t_{i+1}, t_{i+2}]$

$$\begin{aligned} &= \frac{(t_{i+2} - t_{i+1})^{\lambda-1} - (t_{i+1} - t_i)^{\lambda-1}}{t_{i+2} - t_i} + \frac{O((t_{i+2} - t_{i+1})^{1+\lambda}) + O((t_{i+1} - t_i)^{1+\lambda})}{t_{i+2} - t_i} \\ &= \frac{N_{im}^{\lambda-1} \delta_m^{\lambda-1} - M_{im}^{\lambda-1} \delta_m^{\lambda-1}}{(N_{im} + M_{im}) \delta_m} + O\left(\frac{(t_{i+2} - t_{i+1})^{1+\lambda}}{t_{i+2} - t_i}\right) + O\left(\frac{(t_{i+1} - t_i)^{1+\lambda}}{t_{i+2} - t_i}\right) \end{aligned}$$

$$= \frac{N_{im}^{\lambda-1} - M_{im}^{\lambda-1}}{N_{im} + M_{im}} \delta_m^{\lambda-2} + O((t_{i+2} - t_{i+1})^\lambda) + O((t_{i+1} - t_i)^\lambda). \quad (20)$$

A similar argument leads to:

$$\psi_i^L[t_{i+1}, t_{i+2}, t_{i+3}] = \frac{P_{im}^{\lambda-1} - N_{im}^{\lambda-1}}{P_{im} + N_{im}} \delta_m^{\lambda-2} + O((t_{i+3} - t_{i+2})^\lambda) + O((t_{i+2} - t_{i+1})^\lambda). \quad (21)$$

Hence by (20) and (21) (for $l = 0, 1$) the third divided differences of ψ_i^L (needed in (14)) read as:

$$\psi_i^L[t_{i+l}, t_{i+l+1}, t_{i+l+2}] = \frac{R_{im(l+1)}^{\lambda-1} - R_{iml}^{\lambda-1}}{R_{im(l+1)} + R_{iml}} \delta_m^{\lambda-2} + O(\delta_m^\lambda). \quad (22)$$

Coupling again (20) and (21) with telescoped $t_{i+3} - t_i = (t_{i+3} - t_{i+2}) + (t_{i+2} - t_{i+1}) + (t_{i+1} - t_i)$ and $0 < (t_{i+l+1} - t_{i+l})(t_{i+3} - t_i)^{-1} < 1$ reduces the fourth divided difference of ψ_i^L into:

$$\psi_i^L[t_i, t_{i+1}, t_{i+2}, t_{i+3}] = \frac{\frac{P_{im}^{\lambda-1} - N_{im}^{\lambda-1}}{P_{im} + N_{im}} - \frac{N_{im}^{\lambda-1} - M_{im}^{\lambda-1}}{N_{im} + M_{im}}}{t_{i+3} - t_i} \delta_m^{\lambda-2} + \sum_{l=0}^2 O\left(\frac{(t_{i+l+1} - t_{i+l})^\lambda}{t_{i+3} - t_i}\right),$$

which ultimately yields $\psi_i^L[t_i, t_{i+1}, t_{i+2}, t_{i+3}]$

$$= \frac{1}{P_{im} + N_{im} + M_{im}} \left(\frac{P_{im}^{\lambda-1} - N_{im}^{\lambda-1}}{P_{im} + N_{im}} - \frac{N_{im}^{\lambda-1} - M_{im}^{\lambda-1}}{N_{im} + M_{im}} \right) \delta_m^{\lambda-3} + O(\delta_m^{\lambda-1}). \quad (23)$$

The proof of (23) relies on $O\left(\frac{(t_{i+l+1} - t_{i+l})^\lambda}{t_{i+3} - t_i}\right) = O((t_{i+l+1} - t_{i+l})^{\lambda-1}) = O(\delta_m^{\lambda-1})$. The second step resorts to more-or-less uniformity (3) of admitted samplings \mathcal{T} for any $\lambda \in [0, 1]$ (as $\lambda - 1 < 0$). However, to keep all constants in $O(\delta_m^{\lambda-1})$ from (23) as independent from each representative of (3) from now on we admit only β_0 -more-or-less uniform samplings for some fixed $0 < \beta_0 \leq 1$ (see Def. 1.3). The latter permits to exploit the inequality $|(t_{i+l+1} - t_{i+l})^{\lambda-1}| \leq \beta_0^{\lambda-1} \delta_m^{\lambda-1}$ to justify (23) with constants in $O(\delta_m^{\lambda-1})$ depending on γ and λ (but not on samplings \mathcal{T}).

Recalling now that $\psi_i^L(t) = a_i t^2 + b_i t + c_i$ over I_i , by (14) we have:

$$\begin{aligned} a_i &= 3\psi_i[t_i, t_{i+1}, t_{i+2}, t_{i+3}], \\ b_i &= 2\psi_i[t_i, t_{i+1}, t_{i+2}] - 2\psi_i[t_i, t_{i+1}, t_{i+2}, t_{i+3}](t_{i+2} + t_{i+1} + t_i), \\ c_i &= \psi_i[t_i, t_{i+1}] - \psi_i[t_i, t_{i+1}, t_{i+2}](t_i + t_{i+1}) + \psi_i[t_i, t_{i+1}, t_{i+2}, t_{i+3}](t_i t_{i+1} + t_{i+1} t_{i+2} + t_i t_{i+2}). \end{aligned} \quad (24)$$

In the next steps both conditions (6) and (7) enforcing $\dot{\psi}_i^L > 0$ (for arbitrary m) are transformed into their *asymptotic analogues* applicable for sufficiently large m (i.e. for Q_m sufficiently dense). This will ultimately complete the proof of Th. 2.1.

In doing so, both conditions (6) and (7) are reformulated into asymptotic counterparts expressed in terms of (M_{im}, N_{im}, P_{im}) (see Th. 2.1). To save space only the first inequality from (6) i.e. $a_i < 0$ is fully addressed here (which automatically covers both (i) and (iv) - see (9) and (12)). The remaining more complicated cases (ii), (iii) and (v) (listed below) are supplemented with the final asymptotic formulas (10), (11) and (13). The proof of the latter shall be given in the full journal version of this paper.

(i) By (24) the first inequality $a_i < 0$ from (6) amounts to $\psi_i^L[t_i, t_{i+1}, t_{i+2}, t_{i+3}] < 0$ which in turn by (23) holds subject to:

$$\left(\frac{P_{im}^{\lambda-1} - N_{im}^{\lambda-1}}{(P_{im} + N_{im})(P_{im} + N_{im} + M_{im})} - \frac{N_{im}^{\lambda-1} - M_{im}^{\lambda-1}}{(N_{im} + M_{im})(P_{im} + N_{im} + M_{im})} \right) \delta_m^{\lambda-3} + O(\delta_m^{\lambda-1}) < 0, \quad (25)$$

for $(M_{im}, N_{im}, P_{im}) \in [\beta_0, 1]^3$. Asymptotically, for fixed $\lambda \in [0, 1)$ the slowest term determining the sign of (25) accompanies $\delta_m^{\lambda-3}$ and reads as (for all β_0 -more-or-less uniform samplings):

$$\theta_1(M_{im}, N_{im}, P_{im}) = \frac{1}{P_{im} + N_{im} + M_{im}} \left(\frac{P_{im}^{\lambda-1} - N_{im}^{\lambda-1}}{P_{im} + N_{im}} - \frac{N_{im}^{\lambda-1} - M_{im}^{\lambda-1}}{N_{im} + M_{im}} \right),$$

provided θ_1 is not of any order $\Theta(\delta_m^{2+\varepsilon})$ with $\varepsilon \geq 0$. A possible sufficient condition guaranteeing the latter is to require:

$$\theta_1(M_{im}, N_{im}, P_{im}) \leq \rho < 0, \quad (26)$$

to hold for any fixed $\rho < 0$. Evidently (26) amounts to the first inequality (9) assumed to hold in Th 2.1 in order to enforce asymptotically the first inequality in (6) (for any fixed $\lambda \in [0, 1)$).

(ii) A similar but longer argument shows that (upon combining (8), (14), (19), (22) and (23)) the asymptotic fulfillment of the second inequality from (6) i.e. $\psi_i^L(t_i) > 0$ is met subject to (10) satisfied for any fixed, but arbitrary small $\rho_1 > 0$ and sufficiently large m .

(iii) The third inequality $\psi_i^L(t_{i+3}) > 0$ determining (6) maps analogously into its asymptotic counterpart (11) assumed to be fulfilled for an arbitrary but fixed $\rho_2 > 0$ and m sufficiently large.

(iv) Clearly the proof of (9) yields a symmetric sufficient condition for $a_i > 0$ (representing the first inequality in (7)) to hold asymptotically. The latter coincides with (12) stipulated to be satisfied by any fixed $\rho_3 > 0$, subject to m getting large.

(v) The reformulation of $\kappa_{im} = \psi_i^L(\frac{-b_i}{2a_i}) > 0$ from (7) into (13) (assumed to hold for any fixed $\rho_4 > 0$ and sufficiently large m) involves a more intricate treatment (it is omitted here). \square

The asymptotic conditions established in Th. 2.1 in the form of specific inequalities depend (for each i) exclusively on triples $(M_{im}, N_{im}, P_{im}) \in [\beta_0, 1]^3$ and fixed $\lambda \in [0, 1)$ (not on curve γ). Consequently, they can all be also visualized geometrically in 3D for each $i = 3k$ and $\lambda \in [0, 1)$ as well as for any regular curve γ . Several examples with 3D plots are presented in Section 3 with the aid of *Mathematica Package* [22].

We note that all asymptotic conditions from Th. 2.1 can be extended to their 2D analogues (with extra argument used establishing in fact a new theorem) which in turn can be visualized in more appealing 2D plots. Again it is omitted here as exceeding the scope of this paper.

Recall that *uniform sampling*, for which $M_{im} = N_{im} = P_{im} = 1$ (i.e. where $\beta_0 = 1$) combined with $\lambda \in [0, 1)$ or $\lambda = 1$ with (1) both yield $\psi_i^L = 1 + O(\delta_m^2) > 0$ (see [9] and [19])). Noticeably, conditions (10), (11) and (13) are met for either $\lambda = 1$ or \mathcal{T} uniform and $\lambda \in [0, 1)$. In contrast none of (9) or (12) (participating in either (6) or (7)) holds for the above two eventualities. A possible remedy to incorporate these two special cases in adjusted asymptotic representations of either $a_i > 0$ or $a_i < 0$ is to apply the fourth-order Taylor expansion for $\gamma \in C^4$ - see (16). The analysis (left out here) yields a modified condition for $a_i > 0$ (and thus for $a_i < 0$), this time hinging not only on triples $(M_{im}, N_{im}, P_{im}) \in [\beta_0, 1]^3$, $\lambda \in [0, 1)$ but also on γ curvature $\|\ddot{\gamma}(t_i)\|^2$ along \mathcal{T} (see [9] and [19]) - here $\|\dot{\gamma}(t)\| = 1$ as γ is a regular curve and as such can be assumed to be parameterized by arc-length (see [2]). The latter may not always be given in advance. Alternatively, one could rely on *a priori* imposed restrictions on curvatures of γ belonging to the prescribed family of admissible curves.

3 Experimentation and Testing

In this section first Th. 2.1 is illustrated with some examples based on algebraic tests supported by 3D plots generated in *Mathematica* (see Subsection 3.1). Next the convergence rate $\alpha(\lambda)$ for

$d(\gamma) - d(\hat{\gamma}^L) = O(\delta_m^{\alpha(\lambda)})$ is numerically investigated. A special attention is given to $\lambda \in [0, 1]$ yielding ψ^L as a piecewise C^∞ reparameterization of $[0, T]$ into $[0, \hat{T}]$ (see Subsection 3.2).

In doing so, in a preliminary step, for a given fixed β_0 two families of β_0 -more-or-less uniform samplings (27) and (29) are introduced. Next the fulfillment of the asymptotic sufficient conditions enforcing the injectivity of $\psi^L > 0$ (see Th. 2.1) is examined for various $\lambda \in [0, 1]$ and both samplings (27) and (29). In particular, the inequalities (9), (10), (11), (denoted in this section by (6)*) and (12), (13) (marked here with (7)*) representing asymptotically in 3D both (6) and (7) are tested for different sets of triples $(M_{im}, N_{im}, P_{im}) \in [\beta_0, 1]^3$ characterizing either (27) or (29). The algebraic calculations performed herein (assuming m is sufficiently large) are supplemented by geometrical visualizations with 3D plots in *Mathematica*. At this point, we re-emphasize that the asymptotic conditions from Th. 2.1 can be extended further into respective 2D counterparts upon some laborious calculations. In return, the latter gives some advantage in visualizing more appealing 2D (*versus* 3D) plots. To save the space the relevant theory and testing concerning this extra 2D case are left out here.

The second example reports on tests designed to numerically evaluate $\alpha(\lambda)$ in length estimation $d(\gamma) - d(\hat{\gamma}^L) = O(\delta_m^{\alpha(\lambda)})$, for any $\lambda \in [0, 1]$ yielding each ψ_i^L as an injective function. The conjecture concerning $\alpha(\lambda)$ is proposed in Rem. 3.2 based on our numerical results.

The tests reported here are performed for 2D and 3D curves γ_{sp}, γ_S introduced in Ex. 2 (i.e. for $n = 2, 3$). However all established results with the accompanied experimentation are equally applicable to arbitrary multidimensional reduced data $Q_m = \{q_i\}_{i=0}^m$ with $q_i = \gamma(t_i) \in \mathbb{E}^n$.

3.1 Testing Injectivity of ψ^L

Example 1. Consider first the following family \mathcal{T}_1 of *more-or-less uniform sampling* (for geometrical distribution of $\{\gamma(t_i)\}_{i=0}^{15}$ with sampling (27) see also Fig. 3 a) and Fig. 4 a)):

$$t_i = \begin{cases} \frac{i}{m} + \frac{1}{2m}, & \text{for } i = 4k + 1, \\ \frac{i}{m} - \frac{1}{2m}, & \text{for } i = 4k + 3, \\ \frac{i}{m}, & \text{for } i = 2k, \end{cases} \quad (27)$$

for which $K_l = \frac{1}{2}$, $K_u = \frac{3}{2}$ and $\beta_1 = \frac{1}{3}$ (see Def. 1.2). Here $0 \leq i \leq m = 3k$, where $k \in \{1, 2, \dots\}$, so that $t_0 = 0$ and $t_m = T = 1$. Upon resorting to (8) the following 3D compact asymptotic representation \mathcal{T}_1^{3D} of \mathcal{T}_1 reads as (for $m = 3k$):

$$\mathcal{T}_1^{3D} = \left\{ \left(1, \frac{1}{3}, \frac{1}{3}\right), \left(1, 1, \frac{1}{3}\right), \left(\frac{1}{3}, 1, 1\right), \left(\frac{1}{3}, \frac{1}{3}, 1\right), \left(1, \frac{1}{3}, \frac{2}{3}\right), \left(\frac{1}{3}, 1, \frac{2}{3}\right) \right\}. \quad (28)$$

The last two points in (28) are generated for $m = 3k$ as $t_m = 1$. We set $\beta_0 = 0.16$ and hence as $\beta_0 \leq \beta_1$ the sampling (27) is also β_0 -more-or-less uniform.

We also admit another β_0 -more-or-less uniform sampling \mathcal{T}_2 defined according to (for geometrical spread of $\{\gamma(t_i)\}_{i=0}^{15}$ with sampling (29) see also Fig. 3 b) and Fig. 4 b)):

$$t_i = \frac{i}{m} + \frac{(-1)^{i+1}}{3m}, \quad (29)$$

with $K_l = \frac{1}{3}$, $K_u = \frac{5}{3}$ and $\beta_2 = \frac{1}{5} \geq \beta_0$ (see Def. 1.2). Again we set $t_0 = 0$ and $t_m = T = 1$ with $0 \leq i \leq m = 3k$, for $k \in \{1, 2, \dots\}$. By (8) the 3D asymptotic form \mathcal{T}_2^{3D} of (29) reads as:

$$\mathcal{T}_2^{3D} = \left\{ \left(\frac{4}{5}, \frac{1}{5}, 1\right), \left(\frac{1}{5}, 1, \frac{1}{5}\right), \left(1, \frac{1}{5}, 1\right), \left(1, \frac{1}{5}, \frac{4}{5}\right), \left(\frac{1}{5}, 1, \frac{2}{5}\right) \right\}. \quad (30)$$

The last two points in (30) come for $m = 3k$ as $t_m = 1$ and the first point is due to $t_0 = 0$.

λ	$\lambda = 0.3$		$\lambda = 0.9$	
Conditions	(6)*	(7)*	(6)*	(7)*
Sampling \mathcal{T}_1^{3D}				
$(1, \frac{1}{3}, \frac{1}{3})$	F	F	T	F
$(1, 1, \frac{1}{3})$	F	T	F	T
$(\frac{1}{3}, 1, 1)$	F	T	F	T
$(\frac{1}{3}, \frac{1}{3}, 1)$	F	F	T	F
$(1, \frac{1}{3}, \frac{2}{3})$	F	F	T	F
$(\frac{1}{3}, 1, \frac{2}{3})$	F	T	F	T

Table 1: Testing conditions (6) and (7) (implied asymptotically by (6)* and (7)*) for sampling (27) (represented by (28)) and for $\lambda = 0.3$ and $\lambda = 0.9$ with $\rho = -0.001$, $\rho_1 = 0.05$, $\rho_2 = 0.05$, $\rho_3 = 0.001$ and $\rho_4 = 0.005$. Here **T** stands for *true* and **F** for *false*, respectively.

λ	$\lambda = 0.3$		$\lambda = 0.9$	
Conditions	(6)*	(7)*	(6)*	(7)*
Sampling \mathcal{T}_2^{3D}				
$(\frac{4}{5}, \frac{1}{5}, 1)$	F	F	T	F
$(\frac{1}{5}, 1, \frac{1}{5})$	F	T	F	T
$(1, \frac{1}{5}, 1)$	F	F	T	F
$(1, \frac{1}{5}, \frac{4}{5})$	F	F	T	F
$(\frac{1}{5}, 1, \frac{2}{5})$	F	T	F	T

Table 2: Testing conditions (6) and (7) (implied asymptotically by (6)* and (7)*) for sampling (29) (represented by (30)) and for $\lambda = 0.3$ and $\lambda = 0.9$ with $\rho = -0.001$, $\rho_1 = 0.05$, $\rho_2 = 0.05$, $\rho_3 = 0.001$ and $\rho_4 = 0.005$. Here **T** stands for *true* and **F** for *false*, respectively.

The inequalities (9), (10), (11) marked as (6)* (or (12) and (13) denoted by (7)*) enforcing asymptotically (6) (or (7)) to hold are tested over $[\beta_0, 1]^3$ for both samplings (27) and (29). The fixed parameter λ is set either to $\lambda = 0.3$ or to $\lambda = 0.9$ with $\rho = -0.001$, $\rho_1 = \rho_2 = 0.05$, $\rho_3 = 0.001$ and $\rho_4 = 0.005$ - see Tab. 1 and Tab. 2. The corresponding sets of triples $(M_{im}, N_{im}, P_{im}) \in [\beta_0, 1]^3$ satisfying either (6)* or (7)* represent the respective solids $D_{\beta_0}^\lambda \subset [\beta_0, 1]^3$ plotted in 3D by *Mathematica* as shown in Fig. 1 and Fig. 2.

Noticeably different points from \mathcal{T}_k^{3D} , for $k = 1, 2$ may interchangeably satisfy one of the sufficient conditions enforcing either (6) or (7) to hold asymptotically. The latter is demonstrated in Tab. 1 and Tab. 2. Indeed for $\lambda = 0.3$ all conditions from (6)* are not satisfied by both \mathcal{T}_k^{3D} (for $k = 1, 2$) as we have **F** in the respective columns of both Tab. 1 and Tab. 2. Moreover, the conditions from (7)* are only fulfilled by some points (not all) from \mathcal{T}_k^{3D} . Consequently the injectivity of ψ_i^L for either \mathcal{T}_1^{3D} or \mathcal{T}_2^{3D} is not guaranteed. Geometrically both \mathcal{T}_k^{3D} (for $k = 1, 2$) are not contained in the respective injectivity zones $D_{\beta_0}^{\lambda=0.3}$ (for either (6)* or (7)*). In contrast for $\lambda = 0.9$, a simple inspection of Tab. 1 and Tab. 2 reveals that all points from \mathcal{T}_k^{3D} (for $k = 1, 2$) can be split into two subsets each contained in the injectivity zones $D_{\beta_0}^{\lambda=0.9}$ determined by either (6)* or by (7)*, respectively. Algebraically the latter yields at least one **T** in the last two columns of all rows for both Tab. 1 and Tab. 2. \square

Remark 3.1. Note that if for a given family of β_0 -more-or-less uniform samplings \mathcal{T}_{β_0} the subfamily $\mathcal{T}_{\beta_0}^\nu \subset \mathcal{T}_{\beta_0}$ with extra constraints $\nu_1 \leq M_{im} \leq \nu_2$, $\nu_3 \leq N_{im} \leq \nu_4$ and $\nu_5 \leq P_{im} \leq \nu_6$ (here $\nu = (\nu_1, \nu_2, \nu_3, \nu_4, \nu_5, \nu_6)$) is chosen one can also examine (for a fixed $\lambda \in [0, 1)$) whether $I_\nu^{3D} \subset D_{\beta_0}^\lambda$, where $I_\nu^{3D} = (\nu_1, \nu_2) \times (\nu_3, \nu_4) \times (\nu_5, \nu_6)$. By Th. 2.1, should the latter holds

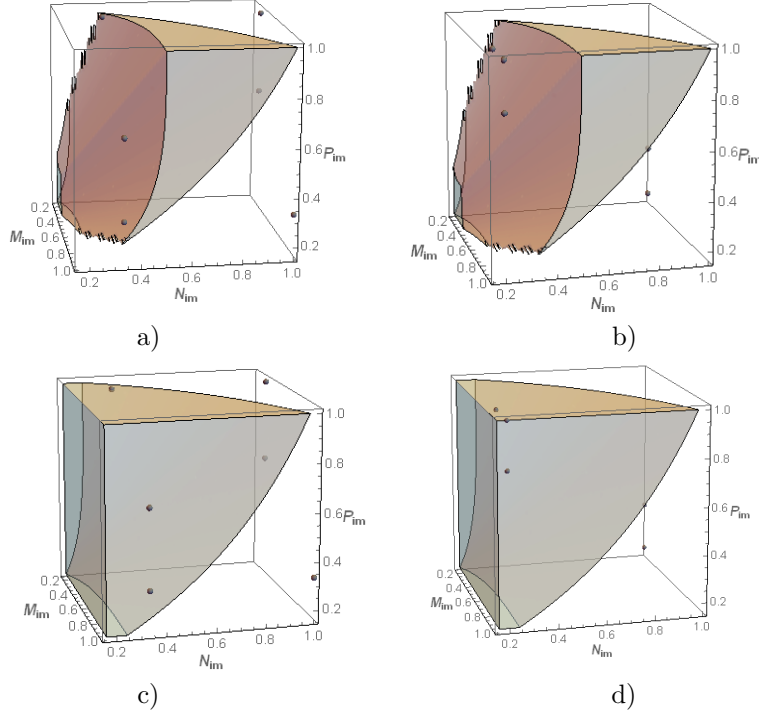


Figure 1: Condition (6) enforced asymptotically by (6)* visualized in 3D plots as two solids $D_{\beta_0}^\lambda \subset [\beta_0, 1]^3$, for $\lambda=0.3$ or $\lambda=0.9$, respectively. Here $\beta_0=0.16$ with dotted points representing samplings: a) (27) mapped into (28) or b) (29) mapped into (30) both for $\lambda=0.3$ and samplings: c) (27) mapped into (28) or d) (29) mapped into (30) both for $\lambda=0.9$.

the entire subfamily of $\mathcal{T}_{\beta_0}^\nu$ yields asymptotically ψ_t^L as injective functions. The incomplete information on input samplings \mathcal{T} carried by $\mathcal{T}_{\beta_0}^\nu$ can in certain situations accompany Q_m . \square

3.2 Numerical testing for length estimation

We pass now to the experiments designed to investigate convergence rate $\alpha(\lambda)$ in length approximation by examining $d(\gamma) - d(\hat{\gamma}) = O(\delta^{\alpha(\lambda)})$ - see Def. 1.3. The coefficient $\alpha(\lambda)$ is estimated numerically by $\tilde{\alpha}(\lambda)$ which in turn is computed using a *linear regression* on the pairs $\{(\log(m), -\log(E_m))\}_{m=m_{min}^{max}}$, where $E_m = |d(\gamma) - d(\hat{\gamma}^L)|$, for a given m . The slope a of the regression line $y(x) = ax + b$ found in *Mathematica* with the aid of `Normal[LinearModelFit[data]]` yields $a = \tilde{\alpha}(\lambda)$ forming a numerical estimate of $\alpha(\lambda)$.

Example 2. Consider a 2D spiral $\gamma_{sp} : [0, 1] \rightarrow \mathbb{E}^2$ (a regular curve with $\gamma_{sp}(0) = (-0.2, 0)$ and $\gamma_{sp}(1) = (1.2, 0)$):

$$\gamma_{sp}(t) = ((t + 0.2) \cos(\pi(1 - t)), (t + 0.2) \sin(\pi(1 - t))), \quad (31)$$

and the so-called 3D Steinmetz curve $\gamma_S : [0, 1] \rightarrow \mathbb{E}^3$ (a regular closed curve with $\gamma_S(0) = \gamma_S(1) = (1, 0, 1.2)$ - see a dotted gray point in Fig. 4):

$$\gamma_S(t) = \left(\cos(2\pi t), \sin(2\pi t), \sqrt{1.2^2 - 1.0^2 \sin^2(2\pi t)} \right). \quad (32)$$

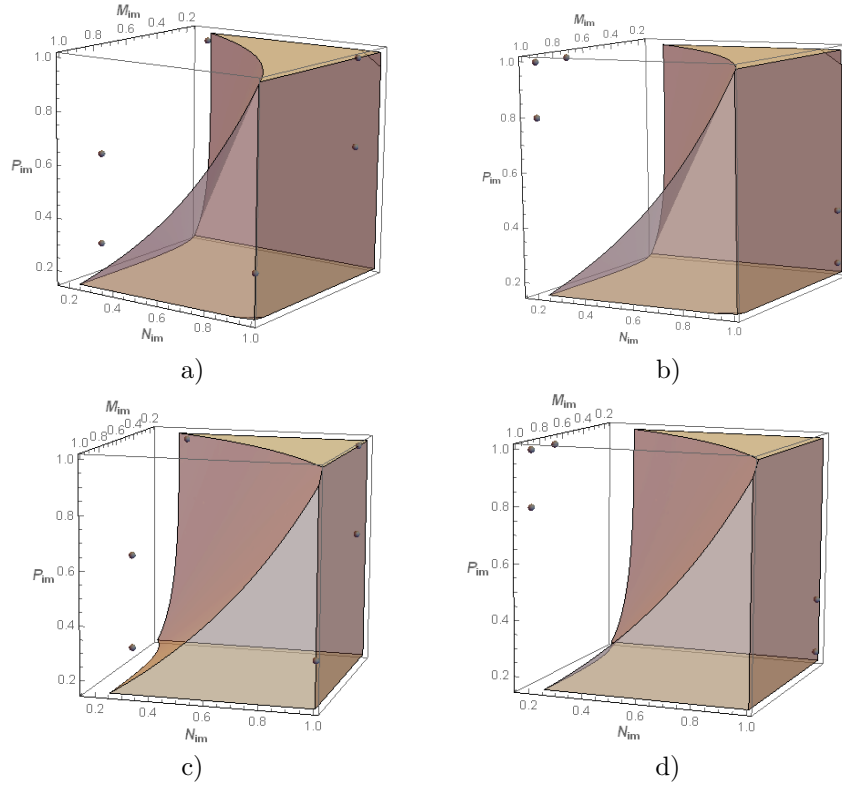


Figure 2: Condition (7) enforced asymptotically by (7)* visualized in 3D plots as two solids $D_{\beta_0}^\lambda \subset [\beta_0, 1]^3$, for $\lambda = 0.3$ or $\lambda = 0.9$, respectively. Here $\beta_0=0.16$ with dotted points representing samplings: a) (27) mapped into (28) or b) (29) mapped into (30) both for $\lambda=0.3$ and samplings: c) (27) mapped into (28) or d) (29) mapped into (30) both for $\lambda=0.9$.

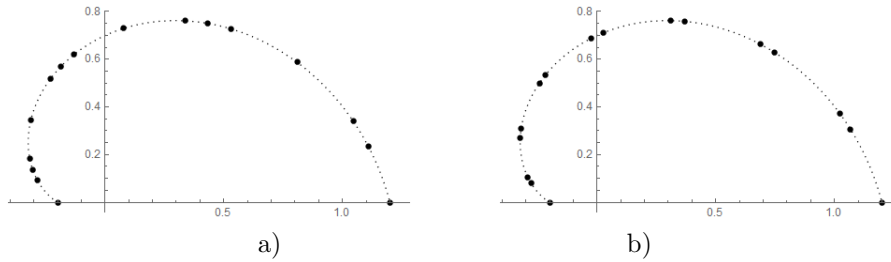


Figure 3: A spiral curve γ_{sp} from (31) sampled according to: a) (27) or b) (29), for $m = 15$.

Both curves γ_{sp} , γ_S (from (31) and (32)) sampled according to either (27) or (29) are plotted in Fig. 3 and Fig. 4, respectively. The numerical results assessing the estimate $\tilde{\alpha}(\lambda)$ of $\alpha(\lambda)$ (for $d(\gamma) - d(\hat{\gamma}^L) = O(\delta_m^{\alpha(\lambda)})$) are presented in Tab. 3. Recall that here, a linear regression to compute $\tilde{\alpha}(\lambda)$ is applied to the collections of points $\{(\log(m), -\log(E_m))\}_{m_{min}=120}^{m_{max}=201}$, with $E_m = |d(\gamma) - d(\hat{\gamma}^L)|$ and for various $\lambda \in \{0.3, 0.7, 0.9\}$. The results from Tab. 3 suggest that for all $\lambda \in \{0.3, 0.7, 0.9\}$ rendering $\psi^L > 0$ (e.g. the latter is guaranteed if Th. 2.1 holds) one

may expect $\lim_{m \rightarrow \infty} E_m = 0$ with *the quadratic convergence rate* $\alpha(\lambda) = 2 \approx \tilde{\alpha}(\lambda)$. \square

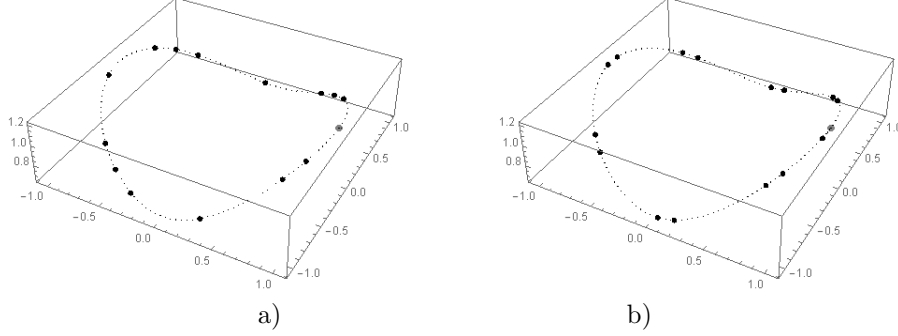


Figure 4: A Steinmetz curve γ_S from (32) sampled according to: a) (27) or b) (29), for $m = 15$ (with dotted gray point $\gamma_S(0) = \gamma_S(1) = (1, 0, 1.2)$).

curve	sampling	λ	$E_{m=201}$	$\alpha(\lambda) \approx \tilde{\alpha}(\lambda)$	(6)* or (7)*
(31)	(27)	0.3	0.0735200	0.044	F
		0.7	0.0000083	1.945	T
		0.9	0.0000016	1.885	T
	(29)	0.3	2.4619100	-0.012	F
		0.7	0.0050445	0.007	F
		0.9	0.0000319	1.989	T
(32)	(27)	0.3	0.2036000	0.033	F
		0.7	0.0000897	2.015	T
		0.9	0.0000181	2.092	T
	(29)	0.3	6.7392400	-0.009	F
		0.7	0.0132964	-0.080	F
		0.9	0.0003419	1.985	T

Table 3: The numerical estimates of $\alpha(\lambda) \approx \tilde{\alpha}(\lambda)$ for a spiral γ_{sp} from (31) and a Steinmetz curve γ_S from (32) computed for $m_{min} = 120 \leq m \leq m_{max} = 201$ and $\lambda \in \{0.3, 0.7, 0.9\}$. Here **T** stands for *true* and **F** for *false*, respectively.

In fact the numerical results from Ex. 2 combined with (5) in conjunction with the argument used to prove $d(\gamma) - d(\hat{\gamma}^L) = O(\delta_m^4)$ for $\lambda = 1$ (see [7] or [19]) lead to expect $\alpha(\lambda) = 2$ in $d(\gamma) - d(\hat{\gamma}^L) = O(\delta_m^{\alpha(\lambda)})$, for all $\lambda \in [0, 1)$ yielding ψ^L as a piecewise C^∞ reparametrization. The latter forms an open problem which can be stated as:

Remark 3.2. Assume $\gamma \in C^4([0, T])$ be a regular curve in \mathbb{E}^n sampled more-or-less uniformly (see Def. 1.2). For the interpolant $\hat{\gamma}^L$ and any $\lambda \in [0, 1)$ in (3) yielding each $\psi_i^L : I \rightarrow \hat{I}$ as a C^∞ genuine reparameterization Ex. 2 suggests a *sharp quadratic convergence rate* in:

$$d(\gamma) - d(\hat{\gamma}_i^L \circ \psi_i^L) = O(\delta_m^2). \quad (33)$$

In particular if Th. 2.1 holds (and β_0 -more-or-less uniform samplings are used) the mapping ψ^L is asymptotically a reparameterization which in turn hints to expect (33). Recall that by *sharpness* of (33) we understand the existence of at least one regular curve of class C^4 and of

at least one samplings from \mathcal{T}_{β_0} such that in (33) the convergence rate $\alpha(\lambda)$ has exactly order 2 (i.e. is not faster than quadratic). \square

4 Conclusions

Fitting reduced data (see e.g. [3] or [16]) constitutes an important task in computer vision and graphics, engineering, microbiology, physics and other applications like medical image processing (e.g. for area, length and boundary estimation or trajectory planning) - see e.g. [4], [6], [8], [11], [14], [15], [17], [20] or [21].

Two sufficient conditions (6) and (7) are first formulated to ensure that the Lagrange piecewise-cubic $\psi^L : [0, T] \rightarrow [0, \hat{T}]$ (introduced in Section 1) is a genuine *reparameterization*. The latter applies to both sparse and dense reduced data Q_m . Here the unknown interpolation knots \mathcal{T} are replaced by $\hat{\mathcal{T}}$ which in turn is determined by exponential parameterization (3) controlled by a single parameter $\lambda \in [0, 1]$ and Q_m . The main contribution established in Th. 2.1 (see Section 2) reformulates (6) and (7) into respective asymptotic representatives valid for sufficiently large m (i.e. for Q_m getting denser). These new transformed conditions (specified in Th. 2.1) depend exclusively on $\lambda \in [0, 1]$ and \mathcal{T} characterized by (8) within the admitted class of β_0 -more-or-less uniform samplings (see Def. 1.2) and apply to any regular curve $\gamma \in C^3([0, T])$ (with $0 < T < \infty$). Lastly, in Section 3 two illustrative examples are presented. The attached 3D plots generated in *Mathematica* [22] illustrate the algebraic character of the asymptotic conditions justified in Th. 2.1 (see Ex. 1). In addition, the numerical examination of the convergence rate in length estimation of interpolated γ for $\lambda \in \{0.3, 0.7, 0.9\}$ are performed. Consequently, based on the latter the conjecture suggesting the quadratic convergence rate for $d(\gamma) - d(\hat{\gamma}^L) = O(\delta_m^2)$ is posed (see Ex. 2 and Rem. 3.2), subject to the injectivity of ψ^L . At this point we remark that all asymptotic formulas from Th. 2.1 are extendable to the corresponding inequalities expressed in (x, y) -variables. This can be achieved by converting first (with the aid of special *homogeneous mapping*) each triple (M_{im}, N_{im}, P_{im}) from (8) into a pair $(x(M_{im}, N_{im}, P_{im}), y(M_{im}, N_{im}, P_{im}))$ and then by reformulating all conditions from Th. 2.1, accordingly in terms of (x, y) . The satisfaction of such new conditions enforces (9), (10) and (11) or (12) and (13) asymptotically (and thus of (6) or (7)). It is a big advantage to reduce the illustrations from 3D to more appealing 2D analogues. We omit here the theoretical discussion and the geometrical insight of this 2D extension of Th. 2.1. Similarly, recall that only items (i) and (iv) (see Section 2) are given here a full proof. In contrast, the final steps of proving (ii), (iii) and (v) are left out as treated later exhaustively in a journal version of this work (together with the mentioned above 2D extension of Th. 2.1).

Future work may include various interpolation schemes $\hat{\gamma}$ or ϕ based on Q_m combined with either (3) or with other $\hat{\mathcal{T}}$ compensating the unknown knots \mathcal{T} (see e.g. [3], [10], [13] or [16]). Searching for alternative sufficient conditions enforcing ψ_i^L to be injective forms an interesting topic. Lastly the theoretical justification of (33) poses another open problem. —

References

- [1] C. de Boor. *A Practical Guide to Spline*. Springer, 1985. https://www.researchgate.net/publication/200744645_A_Practical_Guide_to_Spline.
- [2] M.P. do Carmo. *Differential Geometry of Curves and Surfaces*. Prentice-Hall, 1976. <http://www2.ing.unipi.it/griff/files/dC.pdf>.
- [3] M.P. Epstein. On the influence of parameterization in parametric interpolation. *SIAM J. Numer. Anal.*, 13(2):261–268, 1976. <https://doi.org/10.1137/0713025>.

- [4] G. Farin. *Curves and Surfaces for Computer Aided Geometric Design*. Academic Press, 1993. <https://www.sciencedirect.com/book/9780122490521/curves-and-surfaces-for-computer-aided-geometric-design>.
- [5] M.S. Floater. Chordal cubic spline interpolation is fourth-order accurate. *IMA J. Numer. Anal.*, 25(1):25–33, 2005. <https://doi.org/10.1093/imanum/dri022>.
- [6] M. Janik, R. Kozera, and P. Koziol. Reduced data for curve modeling - applications in graphics, computer vision and physics. *Adv. Sci. Technol. Res. J.*, 7(18):28–35, 2013. <https://doi.org/10.5604/20804075.1049599>.
- [7] R. Kozera. Curve modeling via interpolation based on multidimensional reduced data. *Studia Informaticae*, 25(4B(61)):1–140, 2004. http://dx.doi.org/10.21936/si2004_v25.n4B.
- [8] R. Kozera and M. Wilkołazka. A natural spline interpolation and exponential parameterization for length estimation of curves. *Proc. Amer. Inst. Physics*, 1863(1):400010–1–400010–4, 2017. <https://doi.org/10.1063/1.4992579>.
- [9] R. Kozera and M. Wilkołazka. Convergence order in trajectory estimation by piecewise cubics and exponential parameterization. *Math. Model. Anal.*, 24(1):72–94, 2019. <https://doi.org/10.3846/mma.2019.006>.
- [10] R. Kozera and M. Wilkołazka. A note on modified Hermite interpolation. *Math. Comput. Sci*, 2019. <https://doi.org/10.1007/s11786-019-00434-3>.
- [11] R. Kozera and L. Noakes. C^1 interpolation with cumulative chord cubics. *Fundam. Inform.*, 61(3):285–301, 2004. <https://dl.acm.org/doi/abs/10.5555/1031956.1031962>.
- [12] R. Kozera and L. Noakes. Piecewise-quadratics and exponential parameterization for reduced data. *Appl. Math. Comput.*, 221:620–638, 2013. <https://doi.org/10.1016/j.amc.2013.06.060>.
- [13] R. Kozera and L. Noakes. Piecewise-quadratics and reparameterizations for interpolating reduced data. *Lect. Notes Comp. Sc.*, 9301:260–274, 2015. https://doi.org/10.1007/978-3-319-24021-3_20.
- [14] R. Kozera, L. Noakes, and M. Wilkołazka. A modified complete spline interpolation and exponential parameterization. *Lect. Notes Comp. Sc.*, 9339:98–110, 2015. https://doi.org/10.1007/978-3-319-24369-6_8.
- [15] R. Kozera, L. Noakes, and P. Szmielew. Convergence orders in length estimation with exponential parameterization and ε -uniformly sampled reduced data. *Appl. Math. Inf. Sci.*, 10(1):107–115, 2016. <http://dx.doi.org/10.18576/amis/100110/>.
- [16] E.B. Kuznetsov and A.Y. Yakimovich. The best parameterization for parametric interpolation. *J. Comput. Appl. Math.*, 191(2):239–245, 2006. <https://core.ac.uk/download/pdf/81959885.pdf>.
- [17] B.I. Kvasov. *Methods of Shape-Preserving Spline Approximation*. World Scientific Publishing Company, 2000. <https://doi.org/10.1142/4172>.
- [18] E.T.Y. Lee. Choosing nodes in parametric curve interpolation. *Comput.-Aided Des.*, 21(6):363–370, 1989. [https://doi.org/10.1016/0010-4485\(89\)90003-1](https://doi.org/10.1016/0010-4485(89)90003-1).
- [19] L. Noakes and R. Kozera. Cumulative chords piecewise-quadratics and piecewise-cubics. In R. Klette, R. Kozera, L. Noakes, and J. Weickert, editors, *Geometric Properties of Incomplete Data, Computational Imaging and Vision*, volume 31, chapter 4, pages 59–75. Springer, Dordrecht, 2006. https://link.springer.com/chapter/10.1007/1-4020-3858-8_4.
- [20] L. Piegl and W. Tiller. *The NURBS Book*. Springer-Verlag, 1997. <https://link.springer.com/book/10.1007/978-3-642-59223-2>.
- [21] A. Rababah. High order approximation methods for curves. *Comput.-Aided Geom. Design*, 12(1):89–102, 1995. [https://doi.org/10.1016/0167-8396\(94\)00004-C](https://doi.org/10.1016/0167-8396(94)00004-C).
- [22] S. Wolfram. *The Mathematica Book*. Wolfram Media Inc., 2003. <https://www.wolfram.com/books/profile.cgi?id=4939>.